Photoinduced Forward and Backward Pedalo-Type Motion of a Molecular Switch

Conti, I.; Buma, W.J.; Garavelli, M.; Amirjalayer, S.

DOI
10.1021/acs.jpclett.0c01094

Publication date
2020

Document Version
Final published version

Published in
Journal of Physical Chemistry Letters

THE JOURNAL OF PHYSICAL CHEMISTRY Letters

pubs.acs.org/JPCL Letter

Photoinduced Forward and Backward Pedalo-Type Motion of a Molecular Switch

Irene Conti, Wybren Jan Buma, Marco Garavelli,* and Saeed Amirjalayer*

Cite This: J. Phys. Chem. Lett. 2020, 11, 4741−4746 Read Online

ACCESS | Metrics & More | Article Recommendations | Supporting Information

ABSTRACT: Photoresponsive molecular switches enable spatial and temporal control of molecular processes and are therefore crucial for the development of smart functional materials. Because the light-induced dynamics of these switching units are at the core of the resulting functionality, a detailed insight into their structural time evolution is fundamental for molecular embedding. Here, we performed a hybrid quantum mechanics (CASPT2 and TDDFT)/molecular mechanics (QM/MM) study to elucidate the photodynamics of an azodicarboxamide-based molecular switch, which is a promising candidate for implementation in highly dense environments such as polymers. In particular, we report a detailed picture of the molecular motion at the atomic level based on a relevant number of excited-state trajectories. We show that the azodicarboxamide-based molecular switch undergoes both a forward and backward pedalo-type motion upon excitation. Trans−cis photoisomerization on the other hand, which is well-known to occur for other azo-based chromophores, is shown to be a negligible pathway. By validating the volume-conserving pedalo-type motion, we provide a rational basis for the design of novel types of photoresponsive functional materials in which the active component must operate in a confined space.

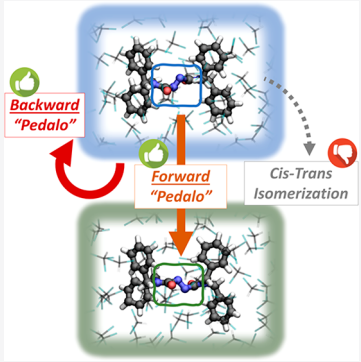

Externally controllable molecular building units are fundamental for the development of responsive functional materials.[1] Using external stimuli to change their properties at the atomic level, such units enable their users to tailor molecular phenomena in a highly controlled manner and transmit these phenomena to the macroscopic world. The potential of these molecular species is well illustrated by considering biological processes where molecular photoresponsive units embedded in a protein environment enable nature to transform light into well-defined functionalities.[2] Tremendous efforts are therefore being made to develop analogous artificial responsive systems using integrated molecular switching units to precisely tune the chemical and physical properties by external stimuli.[3−9] A number of different molecular switching units have thus been synthesized and implemented in functional materials.[10−12] In all these cases, the stimulus-induced structural evolution of the molecular switch is at the basis of the resulting functionality, yet the actual motion at the atomic level is often still a subject of extensive debate.[13] This strongly impedes a rational development of responsive materials for targeted applications. An atomic insight into the dynamics in real time is thus crucial both from fundamental as well as application-driven points of view.

Recently, we introduced a volume-conserving photoinduced motion in a new class of azodicarboxamide-based switching units (Figure 1a).[14−16] This type of motion allows down to implement molecular switching units into sterically hindered and highly constrained molecular environments such as polymers.[16] On the basis of vibrational fingerprints obtained by time-resolved infrared spectroscopy in combination with static density functional theory (DFT) calculations, we concluded that photoexcitation of the azodicarboxamide-molecular switch induced a pedalo-type motion. However, more recently such a motion has been called into question in theoretical studies of Liu and co-workers[17] in which the excited-state dynamics of the bare chromophore in the gas phase and of the chromophore with two water molecules were simulated at the multiconfigurational CASSCF level. In contrast to the pedalo-type motion, they proposed that N=N trans−cis isomerization, known from other azobenzene-based systems,[18−20] takes place. These two types of motions are accompanied by significantly different steric demands and are thus expected to have a dramatic impact on the performance of this class of molecular switching units, in particular when embedded in constrained environments. To resolve this controversy, we have performed extended atomistic dynamical simulations to disentangle the mechanism at work in azodicarboxamide-based molecular switches.

Received: April 8, 2020
Accepted: May 15, 2020
Published: May 15, 2020

https://dx.doi.org/10.1021/acs.jpclett.0c01094
J. Phys. Chem. Lett. 2020, 11, 4741−4746

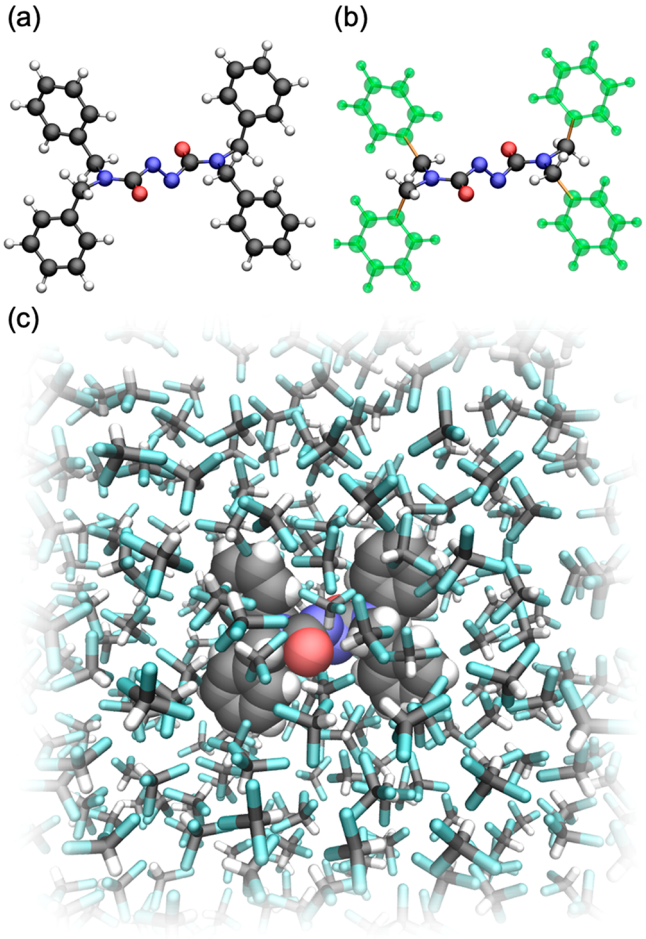

Figure 1. (a) Ball-and-stick model of the azodicarboxamide-based molecular switch. (b) QM and MM region (green) within the molecule. For clarity, the linking bonds are highlighted in orange. (c) Representation of the full hybrid QM/MM model including the explicit chloroform molecules.

We employed a hybrid quantum mechanics/molecular mechanics (QM/MM) approach to describe both the photoactive moiety and its molecular environment. To this purpose, we utilized the COBRAMM code,[21] which enables us to couple state-of-the-art *ab initio* methods representing the core unit with an explicit classical atomistic model (Amber force field[22]) of the environment (Figure 1b,c). In this framework, the dynamics of the azodicarboxamide core involved in the electronic excitations is described at the QM level while the four azodicarboxamide phenyl substituents and the molecular embedding are represented at the MM level (Figure 1b). Notably, and in contrast to previous studies,[16,17] we incorporated solvation effects by including an explicit representation of the chloroform solvent molecules at the MM level (including electrostatic and steric influence, Figure 1c). The importance of the embedding on the excited-state dynamics has been proven previously for a wide range of different systems.[23,24] The QM/MM setup involves three different layers. The QM part (high layer, HL) is described either by the complete active-space second-order perturbation theory (CASPT2(18e,12o)/6-31G*), which allows us to include dynamical correlation effects, whose energy components are fundamental to define the relative excited states energies (Table S1), or at the time dependent-density functional theory (TD-DFT) CAM-B3LYP/6-31G* level.[25] The remaining part is represented by the AMBER force field, where the azodicarboxamide-based molecular switch and the solvent molecules within 9 Å of the solute are movable (medium layer, ML) and the rest of the drop, up to a distance of 15 Å, is frozen at the QM/MM ground-state optimized geometry (low layer, LL) (see the Supporting Information for further computational details).

In order to efficiently perform extended molecular dynamics (MD) simulations that enable covering the full photodynamic process, we initially focused on benchmarking the DFT approach with respect to the multireference method. Geometry optimization of the molecule in its electronic ground state (S_0) showed, in line with previous calculations,[16,17] that the central azodicarboxamide moiety of the molecular switch has a nonplanar configuration. The optimized structural parameters at the CAM-B3LYP and the MP2 level are in very good agreement (Table 1 and Figure 2a).

Table 1. Structural Parameters of the Azodicarboxamide Switch in Its Electronic Ground State (S_0) and First Excited Singlet State (S_1)[a]

	S_0		S_1	
	CAM-B3LYP	MP2	CAM-B3LYP	CASPT2
$C_2-N_3-N_4$	112.3°	110.0°	128.3°	125.8°
$N_3-N_4-C_5$	111.5°	109.7°	124.8°	122.5°
$N_1-C_2-N_3-N_4$	107.0°	103.1°	178.9°	178.8°
$N_3-N_4-C_5-N_6$	121.0°	115.1°	178.3°	176.1°
$C_2-N_3-N_4-C_5$	176.1°	175.9°	179.8°	177.7°

[a]Geometries have been optimized at the QM/MM level, where the QM part corresponds to CAM-B3LYP/6-31G* (S_0 and S_1), MP2/6-31G* (S_0), and CASPT2(18e,12o)/6-31G* (S_1) calculations.

Excited-state calculations lead to a similar conclusion because it was found that the excited-state properties at the CAM-B3LYP and CASPT2 levels are quite comparable, as is clear from calculations of vertical excitation energies, oscillator strengths, and character of the electronic transitions (Table 2 and Figure 2b; Supporting Information Table S1 and Figure S1). Importantly, geometry optimizations of the system in the first excited singlet state (S_1) with either of the two methods resulted in a planar configuration of the azodicarboxamide unit. Comparison of the equilibrium structures obtained at the two levels showed again an excellent agreement (Table 1 and Figure 2c).

Going beyond the stationary points, we calculated the energy profile on the S_0 and S_1 states along the coordinate describing the pedalo-type motion. This pathway consists mainly of a concerted rotation around the two C−N bonds (Figure 3), where the dihedral angles α_{NCNN} (blue) and β_{NNCN} (red) (Figure 2a) are rotated in opposite directions. The profile has been obtained by fixing these two dihedral angles and optimizing the rest of the other structural parameters including those of the solvent. At the CAM-B3LYP level, the S_0 and S_1 energy profiles match well the MP2 and CASPT2 data, respectively (Figure 3). With both methods an out-of-plane energy minimum is calculated in the ground state at about 110° $\alpha_{NCNN}/\beta_{NNCN}$ angle values, while in the first excited singlet state the structure with both torsional angles at 180° represents the energetically preferred geometry. For further discussion it is important to realize that in the electronic

https://dx.doi.org/10.1021/acs.jpclett.0c01094
J. Phys. Chem. Lett. 2020, 11, 4741−4746

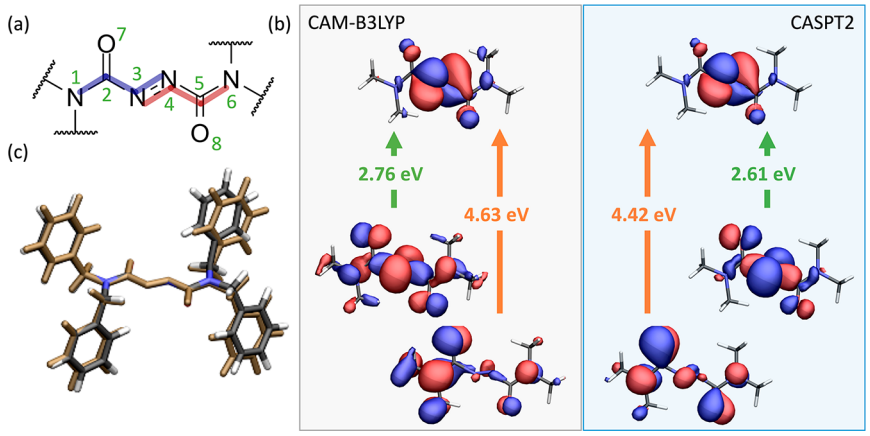

Figure 2. (a) Lewis-structure formula of the azodicarboxamide unit together with the atom numbering used to analyze the structures (see Table 1). (b) Calculated molecular orbitals (largest contributions) involved in the vertical $S_0 \rightarrow S_1$ (orange) and $S_0 \rightarrow S_2$ (green) transitions and the corresponding excitation energies at the CAM-B3LYP (left) and CASPT2 (right) levels. Figure S1 in the Supporting Information shows the full active space, involving π and n type orbitals. (c) Overlay of the geometries optimized in the S_1 state at the CAM-B3LYP and CASPT2 (ochre) levels, respectively.

Table 2. Calculated Vertical Excitation Energies (eV) at the Optimized S_0 Geometry Obtained at the CAM-B3LYP/6-31G* and CASPT2(18e,12o)/6-31G* Levels

	CAM-B3LYP	CASPT2
S_1	2.76	2.61
S_2	4.63	4.42
S_3	4.76	4.52
S_4	5.01	4.44

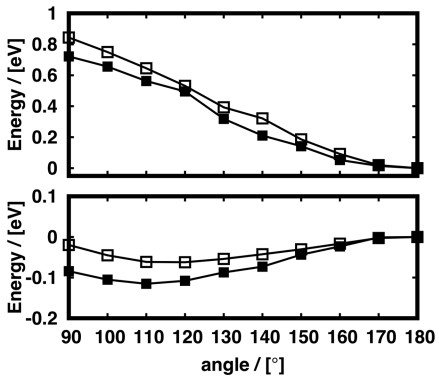

Figure 3. Energy profile along the pedalo-type motion in the electronic ground state S_0 (bottom) and first excited singlet state S_1 (top) optimized at the CAM-B3LYP (open squares) and at the MP2/CASPT2 level (filled squares), respectively. The CASPT2 approach includes numerical gradients at the CASPT2 level. The QM energy is plotted, and for clarity only the absolute angle describing both torsions α_{NCNN} and β_{NNCN} is given (see the Supporting Information for the total energy profile of the QM/MM system).

ground state this structure is associated with an energy maximum along the pedalo-type motion coordinate.

On the basis of these static calculations that validate the DFT and TD-DFT CAM-B3LYP-based QM/MM approach, we performed atomistic simulations to follow the structural behavior and to elucidate the photoinduced switching mechanism. In these simulations thermal effects were incorporated by using a Wigner sampling to generate an ensemble of initial configurations (see the Supporting Information). To compare with the experimental studies in which the system was excited at 355 nm,[16] we ran in total 48 trajectories from the state with the highest oscillator strength among S_1 to S_4 at each configuration. These trajectories demonstrated that this initially excited state shows a rapid electronic internal conversion roughly within a few tens of femtoseconds so that for all practical purposes the relevant structural evolution of the switch occurs on the potential energy surface of the lowest excited singlet state (see Supporting Information Figure S3). We analyzed the structural evolution along each trajectory to decipher the photoinduced dynamics, focusing among others on distinguishing between the pedalo-type motion and the double-bond trans−cis isomerization pathway. To this purpose, we studied the time propagation of the torsion angles around the C−N bonds (α_{NCNN} and β_{NNCN}), which can act as markers for the pedalo-type motion, and the torsional angle γ_{CNNC} around the N−N bond, which is representative for the trans−cis isomerization pathway. From the time evaluation of these structural fingerprints (Figure 4), it is directly evident that the pedalo-type motion is by far the dominating structural relaxation pathway. This clearly supports the operation mechanism proposed on the basis of the time-resolved infrared measurements.[16] Figure 4 shows that the two angles α and β change in opposite directions. Initially, evolution takes places on the potential energy surface of the S_1 state, where in agreement with the static calculations a planarization in the excited state is observed ($\alpha \cong \beta \cong 180°$). Such a motion can be assigned to the first part of the pedalo-type motion and brings the molecule to the planar S_1 minimum from which the S_0/S_1 crossing region is easily accessible. Subsequent structural relaxation on the potential energy surface of the ground state leads to a branching of the population. In about half of the trajectories, the molecular switching unit continues the torsional motion around the C−N bond in a *forward* step (α increasing and β decreasing, Figure 4a), leading to a "photoproduct" formation. The snapshot sequence taken from representative QM/MM trajectories (Figure 4a) provides an atomistic picture of the photoinduced structural evolution of the azodicarboxamide chromophore.

Importantly, we find that for the other half of the population the rotation direction around the C−N bonds is reversed upon relaxation to the ground state, leading effectively to a

https://dx.doi.org/10.1021/acs.jpclett.0c01094
J. Phys. Chem. Lett. 2020, 11, 4741−4746

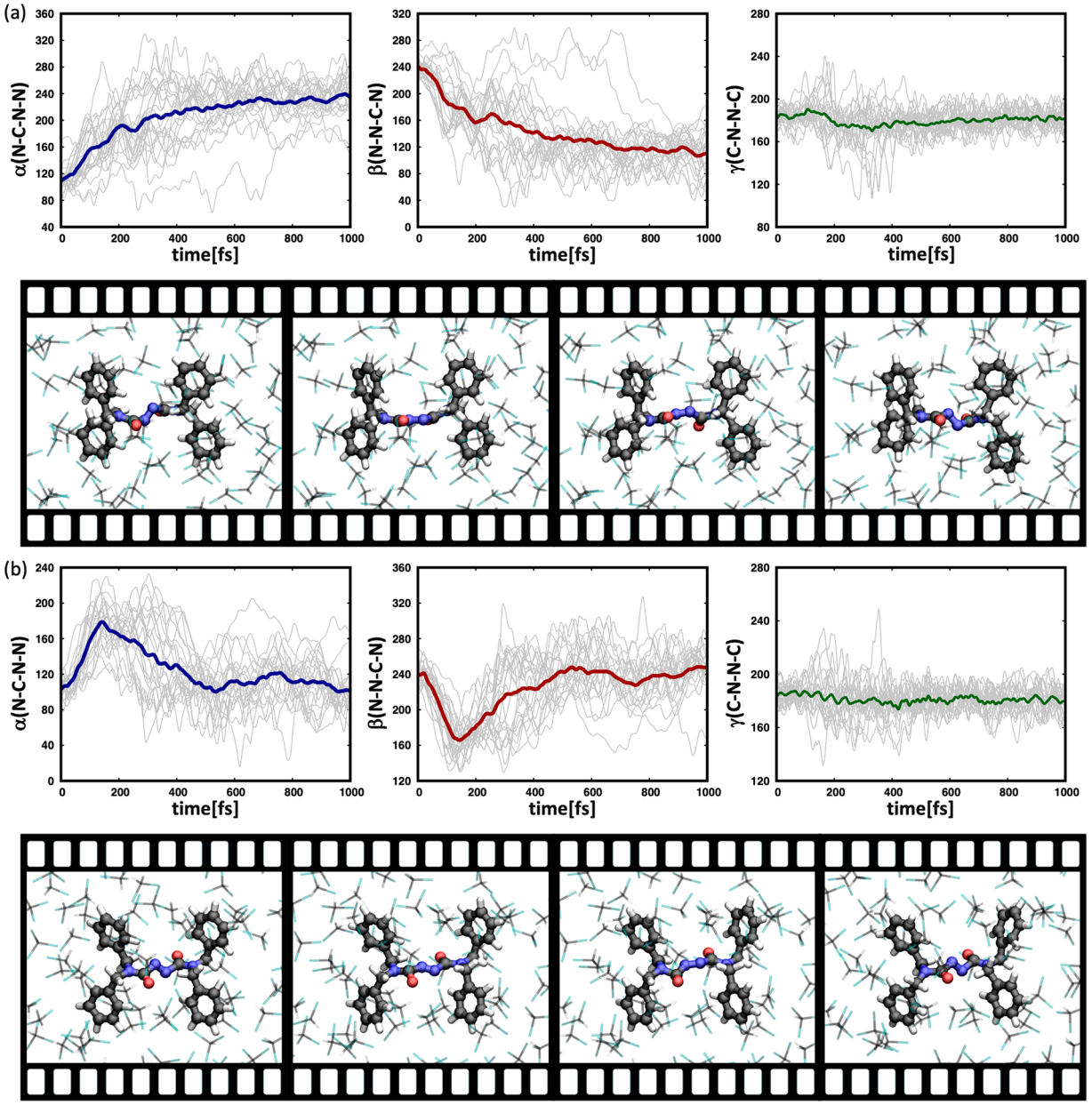

Figure 4. Structural evolution of the torsion angles α_{NCNN}, β_{NNCN}, and γ_{CNNC} extracted from the QM/MM trajectories (top a and b) and snapshots extracted from a representative QM/MM trajectory (bottom a and b) describing (a) the *forward* and (b) the *backward* pedalo-type motion.

backward-motion of the chromophore to the initial configuration (Figure 4b).

To validate the picture derived from the MD simulations and in particular to confirm the relaxation funnel from the electronic excited state to the ground state we optimized the low-lying conical intersections (CIs) between S_1 and S_0 at the CASPT2/MM level (employing numerical gradients at the CASPT2 level).[26,27] Two different CIs for the $S_1 \rightarrow S_0$ transition could be identified whose structural parameters are reported in the Supporting Information (Table S2). The geometry of the first CI is close to the optimized planar S_1 geometry ($\gamma_{CI1} = 175.9°$) and lies about 4.85 kcal/mol above the S_1 minimum. In contrast to this, the second one (CI2) shows a large distortion of the geometry from the planar configuration with a structure in which in particular the C−N−N−C angle is significantly altered ($\gamma_{CI2} = 125.2°$) and is at a slightly higher energy (5.16 kcal/mol above the S_1 minimum). We compared these results with the data obtained from the TD-DFT MD simulations by analyzing for all trajectories the geometry at the $S_1 \rightarrow S_0$ hopping point. Although we used a rather simple criterion to describe the transition between the electronic states in our MD simulations which depends only on the energy gap, a comparison of the average angle ($\gamma_{CAM\text{-}B3LYP(average)} = 161.4°$) with the geometry of the CASPT2 optimized CI1 shows an excellent agreement. We therefore conclude that the dominant relaxation pathway pursued during the excited-state dynamics involves primarily the CI1 funnel.

In addition, because the structural dynamics in S_1 predominantly involve planarization of the azodicarboxamide chromophore, modes involving significant torsional motions around the N=N bond are dynamically disadvantaged along this decay pathway. Therefore, CI2 is expected to be both energetically and even more dynamically less accessible than

https://dx.doi.org/10.1021/acs.jpclett.0c01094
J. Phys. Chem. Lett. 2020, 11, 4741−4746

CI1. Our MD simulations show fewer cases (21 out of 48 trajectories) in which a transition to the ground-state occurs via a region close to the CI2 structure ($\gamma_{CNNC} < 145°$). However, even in these cases they follow the pedalo-type decay mechanism as the driving force in the S_1 state relaxation involves primarily the rotation around the $\alpha_{NCNN}/\beta_{NNCN}$ torsion and not the γ_{CNNC} torsion. The presence of the energy barriers on the potential energy surface of S_1 indicates the possibility to randomize the direction of the pedalo-type motion by modulating the momentum in the excited state before relaxation to the ground state. A detailed analysis of the relevant dihedral angels α_{NCNN} and β_{NNCN} along the trajectory indeed shows an oscillation in the first excited state (Supporting Information Figure S3) and thus supports this hypothesis. Although the detailed topology of the conical intersection might further influence the relaxation pathway, the branching of the population with almost equal yield into forward and backward pedalo-type motion after relaxation to the ground-state is in line with the randomization of the momentum in the excited state. Finally, it should be emphasized that although some structural deformation of γ_{CNNC} is observed along the trajectories, an isomerization pathway by torsion around the N=N bond can be excluded. In fact, only in about 2% (1 out of 48) of our MD simulations was a trans−cis isomerization observed.

This conclusion appears to be at odds with the results reported by Liu et al. where it was concluded that trans−cis isomerization is the main relaxation pathway.[17] However, the discrepancy can be clarified by the fact that the previously employed CASSCF approach fails to accurately describe (a) the potential energy landscape (see Supporting Information Table S1), and consequently also the energetics of the CIs, and (b) the explicit solvent bulk, which could favor a pedalo-type volume-conserving mechanism with respect to a space-demanding cis−trans isomerization process. Our CASPT2 and TDDFT protocol together with the QM/MM approach, which has been successfully employed to model a variety of photoinduced phenomena in organic chromophores,[28,29] indicates that dynamic correlation and an explicit representation of the solvent environment able to model solvent bulk effects, which cover both electrostatic and steric contributions from the solvent surrounding, need to be included for an accurate description of these systems (Table S1) and to deliver an experimentally consistent mechanistic scenario. At the same time, the employed TD-CAM-B3LYP functional, although a single reference approach, accurately reproduces the CASPT2 energy landscape and, consequently, provides an efficient tool to investigate extended azodicarboxamide-based systems at a much cheaper cost.

In summary, using a hybrid QM/MM approach we have been able to come to a detailed description of the structural dynamics occurring upon electronic excitation of azodicarboxamide-based molecular switches under conditions in which they have actually been employed experimentally, which involve an explicit solvent environment. In line with conclusions drawn from time-resolved experimental studies, we find that the dominant relaxation pathway involves a pedalo-type motion. Atomistic simulations in the framework of TD-DFT showed an accurate description of the photoinduced dynamics compared to results calculated at the CASPT2 level. For the presently investigated molecular switch we find that the pedalo-type motion can occur in both a forward and backward direction with about the same yield. It will be interesting to investigate how one could steer the branching ratio, for example, by a judicious choice of substituents or by coherent control.[30,31] Our study provides a strong basis for further exploration of these aspects. Most importantly, our results provide a strong incentive for implementing these classes of azodicarboxamide switching units into confined molecular environments such as polymeric structures.

■ ASSOCIATED CONTENT

Supporting Information

The Supporting Information is available free of charge at https://pubs.acs.org/doi/10.1021/acs.jpclett.0c01094.

Further computational details, vertical energies including CASPT2 active space orbitals and electronic transitions, QM/MM energy profile along the pedalo-type motion coordinate, bright excited-state molecular dynamic simulations, S_0/S_1 conical intersection parameters, and coordinates of critical points (PDF)

■ AUTHOR INFORMATION

Corresponding Authors

Marco Garavelli − *Dipartimento di Chimica Industriale, Università degli Studi di Bologna, 40136 Bologna, Italy;* orcid.org/0000-0002-0796-289X; Email: marco.garavelli@unibo.it

Saeed Amirjalayer − *Physikalisches Institut, Westfälische Wilhelms-Universität Münster, 48149 Münster, Germany; Center for Nanotechnology, 48149 Münster, Germany; Center for Multiscale Theory and Computation, 48149 Münster, Germany;* orcid.org/0000-0003-0777-5004; Email: s.amirjalayer@wwu.de

Authors

Irene Conti − *Dipartimento di Chimica Industriale, Università degli Studi di Bologna, 40136 Bologna, Italy;* orcid.org/0000-0001-7982-4480

Wybren Jan Buma − *Van 't Hoff Institute for Molecular Sciences, University of Amsterdam, 1098 XH Amsterdam, The Netherlands; Institute for Molecules and Materials, FELIX Laboratory, Radboud University, 6525 ED Nijmegen, The Netherlands;* orcid.org/0000-0002-1265-8016

Complete contact information is available at: https://pubs.acs.org/10.1021/acs.jpclett.0c01094

Notes

The authors declare no competing financial interest.

■ ACKNOWLEDGMENTS

We thank Artur Nenov for technical support. This work was further supported by German Research Foundation (DFG) and The Netherlands Organization for Scientific Research (NWO).

■ REFERENCES

(1) Kassem, S.; van Leeuwen, T.; Lubbe, A. S.; Wilson, M. R.; Feringa, B. L.; Leigh, D. A. Artificial molecular motors. *Chem. Soc. Rev.* **2017**, *46* (9), 2592−2621.

(2) Kowalik, L.; Chen, J. K. Illuminating developmental biology through photochemistry. *Nat. Chem. Biol.* **2017**, *13* (6), 587−598.

(3) Yagai, S.; Kitamura, A. Recent advances in photoresponsive supramolecular self-assemblies. *Chem. Soc. Rev.* **2008**, *37* (8), 1520−9.

(4) Yan, X.; Wang, F.; Zheng, B.; Huang, F. Stimuli-responsive supramolecular polymeric materials. *Chem. Soc. Rev.* **2012**, *41* (18), 6042−65.
(5) Qu, D. H.; Wang, Q. C.; Zhang, Q. W.; Ma, X.; Tian, H. Photoresponsive Host-Guest Functional Systems. *Chem. Rev.* **2015**, *115* (15), 7543−88.
(6) Tochitsky, I.; Kienzler, M. A.; Isacoff, E.; Kramer, R. H. Restoring Vision to the Blind with Chemical Photoswitches. *Chem. Rev.* **2018**, *118* (21), 10748−10773.
(7) Tan, P.; Jiang, Y.; Liu, X.-Q.; Sun, L.-B. Making Porous Materials Respond to Visible Light. *ACS Energy Lett.* **2019**, *4* (11), 2656−2667.
(8) Grzelczak, M.; Liz-Marzan, L. M.; Klajn, R. Stimuli-responsive self-assembly of nanoparticles. *Chem. Soc. Rev.* **2019**, *48* (5), 1342−1361.
(9) Kolodzeiski, E.; Amirjalayer, S. Atomistic Insight Into the Host-Guest Interaction of a Photoresponsive Metal-Organic Framework. *Chem. - Eur. J.* **2020**, *26* (6), 1263−1268.
(10) Garcia-Amoros, J.; Velasco, D. Recent advances towards azobenzene-based light-driven real-time information-transmitting materials. *Beilstein J. Org. Chem.* **2012**, *8*, 1003−1017.
(11) Klajn, R. Spiropyran-based dynamic materials. *Chem. Soc. Rev.* **2014**, *43* (1), 148−184.
(12) Strakova, K.; Assies, L.; Goujon, A.; Piazzolla, F.; Humeniuk, H. V.; Matile, S. Dithienothiophenes at Work: Access to Mechanosensitive Fluorescent Probes, Chalcogen-Bonding Catalysis, and Beyond. *Chem. Rev.* **2019**, *119* (19), 10977−11005.
(13) Amirjalayer, S.; Buma, W. J. Light on the Structural Evolution of Photoresponsive Molecular Switches in Electronically Excited States. *Chem. - Eur. J.* **2019**, *25* (25), 6252−6258.
(14) Berna, J.; Alajarin, M.; Orenes, R. A. Azodicarboxamides as Template Binding Motifs for the Building of Hydrogen-Bonded Molecular Shuttles. *J. Am. Chem. Soc.* **2010**, *132* (31), 10741−10747.
(15) Berna, J.; Alajarin, M.; Marin-Rodriguez, C.; Franco-Pujante, C. Redox divergent conversion of a [2]rotaxane into two distinct degenerate partners with different shuttling dynamics. *Chem. Sci.* **2012**, *3* (7), 2314−2320.
(16) Amirjalayer, S.; Martinez-Cuezva, A.; Berna, J.; Woutersen, S.; Buma, W. J. Photoinduced Pedalo-Type Motion in an Azodicarboxamide-Based Molecular Switch. *Angew. Chem., Int. Ed.* **2018**, *57* (7), 1792−1796.
(17) Liu, Y.; Luo, J. Nonadiabatic dynamics simulation of photoisomerization mechanism of photoswitch azodicarboxamide: Hydrogen bonding effects. *J. Photochem. Photobiol., A* **2018**, *367*, 236−239.
(18) Tan, E. M.; Amirjalayer, S.; Smolarek, S.; Vdovin, A.; Zerbetto, F.; Buma, W. J. Fast photodynamics of azobenzene probed by scanning excited-state potential energy surfaces using slow spectroscopy. *Nat. Commun.* **2015**, *6*, 5860.
(19) Nenov, A.; Borrego-Varillas, R.; Oriana, A.; Ganzer, L.; Segatta, F.; Conti, I.; Segarra-Marti, J.; Omachi, J.; Dapor, M.; Taioli, S.; Manzoni, C.; Mukamel, S.; Cerullo, G.; Garavelli, M. UV-Light-Induced Vibrational Coherences: The Key to Understand Kasha Rule Violation in trans-Azobenzene. *J. Phys. Chem. Lett.* **2018**, *9* (7), 1534−1541.
(20) Bockmann, M.; Doltsinis, N. L.; Marx, D. Nonadiabatic hybrid quantum and molecular mechanic simulations of azobenzene photoswitching in bulk liquid environment. *J. Phys. Chem. A* **2010**, *114* (2), 745−54.
(21) Weingart, O.; Nenov, A.; Altoe, P.; Rivalta, I.; Segarra-Marti, J.; Dokukina, I.; Garavelli, M. COBRAMM 2.0 - A software interface for tailoring molecular electronic structure calculations and running nanoscale (QM/MM) simulations. *J. Mol. Model.* **2018**, *24* (9), 271.
(22) Case, D. A., et al. *AMBER 2018*; University of California, San Francisco, 2018.
(23) Teles-Ferreira, D. C.; Conti, I.; Borrego-Varillas, R.; Nenov, A.; Van Stokkum, I. H. M.; Ganzer, L.; Manzoni, C.; de Paula, A. M.; Cerullo, G.; Garavelli, M. A Unified Experimental/Theoretical Description of the Ultrafast Photophysics of Single and Double Thionated Uracils. *Chem. - Eur. J.* **2020**, *26* (1), 336−343.
(24) Nenov, A.; Conti, I.; Borrego-Varillas, R.; Cerullo, G.; Garavelli, M. Linear absorption spectra of solvated thiouracils resolved at the hybrid RASPT2/MM level. *Chem. Phys.* **2018**, *515*, 643−653.
(25) Yanai, T.; Tew, D. P.; Handy, N. C. A new hybrid exchange-correlation functional using the Coulomb-attenuating method (CAM-B3LYP). *Chem. Phys. Lett.* **2004**, *393* (1−3), 51−57.
(26) Bearpark, M. J.; Robb, M. A.; Schlegel, H. B. A Direct Method for the Location of the Lowest Energy Point on a Potential Surface Crossing. *Chem. Phys. Lett.* **1994**, *223* (3), 269−274.
(27) Bearpark, M. J.; Larkin, S. M.; Vreven, T. Searching for conical intersections of potential energy surfaces with the ONIOM method: application to previtamin D. *J. Phys. Chem. A* **2008**, *112* (31), 7286−95.
(28) Conti, I.; Garavelli, M. Evolution of the Excitonic State of DNA Stacked Thymines: Intrabase $\pi\pi^*$ —> S_0 Decay Paths Account for Ultrafast (Subpicosecond) and Longer (>100 ps) Deactivations. *J. Phys. Chem. Lett.* **2018**, *9* (9), 2373−2379.
(29) Giussani, A.; Conti, I.; Nenov, A.; Garavelli, M. Photoinduced formation mechanism of the thymine-thymine (6−4) adduct in DNA; a QM(CASPT2//CASSCF):MM(AMBER) study. *Faraday Discuss.* **2018**, *207* (0), 375−387.
(30) Rabitz, H.; de Vivie-Riedle, R.; Motzkus, M.; Kompa, K. Whither the future of controlling quantum phenomena? *Science* **2000**, *288* (5467), 824−8.
(31) Prokhorenko, V. I.; Nagy, A. M.; Waschuk, S. A.; Brown, L. S.; Birge, R. R.; Miller, R. J. Coherent control of retinal isomerization in bacteriorhodopsin. *Science* **2006**, *313* (5791), 1257−61.

https://dx.doi.org/10.1021/acs.jpclett.0c01094
J. Phys. Chem. Lett. 2020, 11, 4741−4746